2014-10

Stable Doping of Carbon Nanotubes via Molecular Self Assembly

UTD AUTHOR(S): Alex Cook and Anvar A. Zakhidov

Lee, B., Y. Chen, A. Cook, A. Zakhidov, et al. 2014. "Stable doping of carbon nanotubes via molecular self assembly." Journal of Applied Physics 116(144503): 1-5.

Stable doping of carbon nanotubes via molecular self assembly

B. Lee,[1] Y. Chen,[1] A. Cook,[2] A. Zakhidov,[2] and V. Podzorov[1,a)]
[1]*Department of Physics and Institute for Advanced Materials and Devices for Nanotechnology, Rutgers University, New Jersey 08854, USA*
[2]*Department of Physics and NanoTech Institute, University of Texas at Dallas, Richardson, Texas 75083, USA*

(Received 23 July 2014; accepted 29 September 2014; published online 13 October 2014)

We report a novel method for stable doping of carbon nanotubes (CNT) based on methods of molecular self assembly. A conformal growth of a self-assembled monolayer of *fluoroalkyl trichloro-silane* (FTS) at CNT surfaces results in a strong increase of the sheet conductivity of CNT electrodes by 60–300%, depending on the CNT chirality and composition. The charge carrier mobility of undoped partially aligned CNT films was independently estimated in a field-effect transistor geometry ($\sim 100\,cm^2V^{-1}s^{-1}$). The hole density induced by the FTS monolayer in CNT sheets is estimated to be $\sim 1.8 \times 10^{14}\,cm^{-2}$. We also show that FTS doping of CNT anodes greatly improves the performance of organic solar cells. This large and stable doping effect, easily achieved in large-area samples, makes this approach very attractive for applications of CNTs in transparent and flexible electronics. © *2014 AIP Publishing LLC*. [http://dx.doi.org/10.1063/1.4897550]

I. INTRODUCTION

Carbon nanotubes (CNT) have been proposed for applications in chemical and optical sensors,[1–3] transparent electrodes,[4] and field effect transistors (FET).[5–9] A unique method developed by Zhang *et al.*[10] provides a way of fabricating large-area, free-standing or laminated, transparent and partially aligned CNT sheets, creating new possibilities for CNT based technologies. However, in spite of the progress in development of CNT conductors, sheet conductivities, σ, of these systems are still not sufficient to compete with transparent conducting oxides for applications in transparent electronics. This is mainly due to two factors: (a) poor control of the fraction of semiconducting vs. metallic tubes in CNT samples and (b) high electrical resistance associated with interconnects between individual tubes or bundles in CNT networks. Strategies to improve σ include an enrichment of CNT sheets with longer and more oriented individual nanotubes (thus mitigating the problem of interconnects), as well as increasing the fraction of metallic tubes in CNT samples. Here, we propose an interesting alternative approach for improving electrical conductivity of CNTs. Recently developed surface functionalization of semiconductors by self-assembled monolayers (SAM) of *fluoroalkyl trichlorosilanes* (FTS) was shown to result in a very efficient *p*-type doping in a variety of carbon based electronic materials, including small-molecule organic crystals,[11] conjugated polymers[12] and graphene.[13] In this Letter, we report on the growth of FTS self-assembled monolayers on carbon nanotubes and their effect on the electrical properties of CNT sheets.

II. RESULTS AND DISCUSSION

A. Fabrication

Partially aligned and densified CNT sheets were prepared on glass substrates using the method developed by Zhang *et al.*[10] Orientation of the CNT bundles is defined by the fabrication process, in which a quasi two-dimensional network with a preferential CNT alignment is formed over macroscopically large area by pulling entangled CNTs off a wafer covered with a dense CNT "forest". The resultant strong CNT sheets are semi-transparent (transmission in the visible range of spectrum is ~75%) and mainly consist of multi-wall metallic nanotube bundles, which makes the sheet resistivity of as-prepared (undoped) films produced by abovementioned method around $\rho \sim 900\ \Omega/\square$. Electrical contacts were prepared by painting an aqueous suspension of colloidal graphite (Aquadag® E Colloidal Graphite, Ted Pella, Inc., product #16051) on these CNT sheets, defining a macroscopic channel with the typical length, $L = 7$ mm, and width, $W = 5$ mm, with the channel orientation along the CNT alignment. We find that upon drying, the carbon paint makes excellent Ohmic contacts to these CNT samples. The samples were then used for: (a) fabrication and characterization of CNT FETs, and (b) FTS doping.

Top gated field-effect transistors (CNT FETs) were fabricated by depositing a 2 μm-thick *parylene-N* insulating film onto these CNT samples with pre-fabricated graphite contacts, topped with a thermally evaporated 30 nm-thick Ag gate (Fig. 1(a)). Details of the dielectric deposition techniques can be found elsewhere.[14] Figure 1(b) is a photograph of one of the devises. Parylene has been proven to be an excellent gate insulator in FETs based on organic molecular crystals that typically have very smooth and shiny surfaces.[14] In this work, we find that even though densified CNT sheets have a rough nanoscale morphology, with many bundles protruding out of the film, 1–2 μm-thick parylene coating is sufficient to prevent gate-CNT shorts and leakages in our large-area devices, leading to well-behaved FETs. This has been demonstrated in this work by fabrication of top-gated CNT FETs with a negligible gate leakage.

B. Characterization of FET devices

The transfer characteristics of our CNT FETs are shown in Fig. 2. The source-drain current, I_{SD}, was measured as a

a)Electronic mail: podzorov@physics.rutgers.edu.

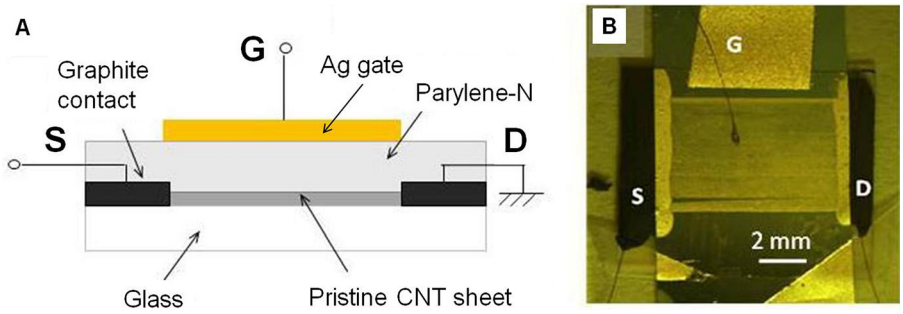

FIG. 1. (a) Schematics of a top-gate FET prepared on aligned large-area CNT sheet densified on glass. Colloidal graphite paint was used for source-drain contacts. A 2 μm-thick parylene-*N* layer ($\varepsilon = 2.6$) deposited on top of the CNT sheet serves as a gate insulator. The gate is a 30 nm-thick Ag film evaporated on top of the parylene-*N*. (b) A photograph (top-view) of an actual large-area CNT FET. The partially aligned CNT array is clearly visible through the semitransparent gate. Outstanding conformal properties of parylene coating allow to avoid gate-channel shorts and leakages, even though the nanoscale morphology of CNT sheets is very rough.

function of the gate voltage, V_G, at different values of the source-drain voltage, V_{SD}. These CNT sheets are already highly conductive even in an ungated state, with their conductivity linearly increasing with V_{SD} (Fig. 2). This background conductivity (represented by the source-drain current at zero V_G, $I_0 \equiv I_{SD}(V_G = 0)$) was subtracted from the corresponding $I_{SD}(V_G)$ curves for clarity. The resultant transfer curves shown in the main panel are highly linear and correspond to a typical *p*-type behavior with a large depletion gate voltage, which is expected for such a conductive material (Fig. 2). The field-effect mobility, μ, was estimated from the slopes of $I_{SD}(V_G)$ dependences using the transconductance equation:

$$\mu = L \cdot |\partial I_{SD}/\partial V_G|/(C_i \cdot V_{SD} \cdot W_{eff}), \qquad (1)$$

where $C_i = 1.1$ nF/cm^2 is the gate-channel capacitance per unit area, and W_{eff} is the effective channel width in our FETs.

Because partially aligned semi-transparent CNT films have sparse nanoscale morphology with many voids between the bundles, the actual (effective) channel width, W_{eff}, might significantly differ from the macroscopic sample's width, W.

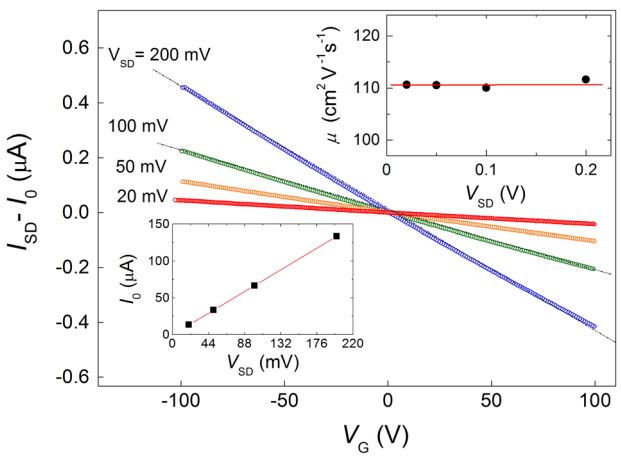

FIG. 2. Transfer characteristics, $I_{SD}(V_G)$, of a typical CNT FET based on partially aligned CNT sheets. For clarity, the off-current (that is, $I_0 \equiv I_{SD}(V_G = 0)$) corresponding to the conductivity of ungated CNT film has been subtracted from each curve. The lower inset: I_0 as a function of V_{SD} that shows an Ohmic relation corresponding to a base-line resistivity of 1 kΩ/□. The upper inset: field-effect mobility μ extracted from the slopes of the transconductance curves at different V_{SD}.

Therefore, instead of treating the sample as a homogeneous two dimensional conductor, a better approach is to consider it as an inhomogeneous film composed of an array of parallel bundles connecting the source and drain contacts with spaces between them. In that case, one should use the effective channel width W_{eff} in Eq. (1) to account for the empty spaces between the bundles. To estimate W_{eff}, we measured optical transmission through our CNT sheets and found that these films are about 75% transparent, suggesting that only 25% of the whole area of the sample is actually covered by CNT bundles, leading to a rough estimate for the effective width of the channel: $W_{eff} \approx 0.25 \times W$. Given the fact that multi-wall CNT bundles are highly absorbing in the visible range, this estimate should not be too far from the actual physical (projected) surface coverage in these samples. With such a correction, a rough estimate for the hole mobility in our CNT FETs, extracted from the data in the main panel of Fig. 2 using Eq. (1), gives $\mu \approx 100\,\text{cm}^2\,\text{V}^{-1}\text{s}^{-1}$, which is V_{SD}-independent in the studied voltage range (Fig. 2). We note that even with the above correction, the extracted mobility should not be taken as the intrinsic mobility of individual nanotubes. This value should be used as an approximate, order-of-magnitude mobility estimate for the purpose of evaluating the doping carrier density. It is worth noting that the transfer characteristics of our devices are highly linear, scale ohmically with V_{SD}, and exhibit negligible hysteresis, which is rarely the case in CNT FETs.[15–17] This indicates that: (a) the contact resistance in our FETs does not represent a major problem, (b) parasitic charge trapping or interfacial charge transfer effects are minimal, and (c) the measurements correctly reflect an average macroscopic mobility of the sparse CNT network in our samples.

C. Doping of CNTs with self-assembled monolayers

Next, we investigated the effect of FTS treatment on the electrical properties of the CNT sheets. Bare CNT samples with contacts were loaded into a dedicated vacuum chamber, which was then pumped down to $<10^{-2}$ Torr, followed by an introduction of FTS vapor. The sheet resistance of the samples has been monitored *in situ* during the exposure to FTS vapor. The typical result is shown in Fig. 3(a). Conductivity of this sample increased by 60% during the first 5 h of doping and saturated after an overnight treatment. Although the

fundamental mechanism of doping induced by FTS SAM in carbon based materials is not yet fully understood, qualitatively the increase of conductivity of CNT sheets upon FTS treatment can be explained by protonic doping.[11–13] Indeed, unbound silanol groups of hydrolyzed FTS molecules forming a two-dimensional polymerized monolayer at the surface of a sample can introduce mobile carriers into the sample, leading to a conductivity increase. Quantitatively, however, the relative effect of FTS treatment on σ is less prominent in these CNT samples (similarly to the case of graphite or graphene[13]), compared to pristine organic semiconductors that are highly insulating in an undoped state and thus exhibit a few orders of magnitude increase of conductivity upon FTS functionalization.[11,12] This is not surprising, because as-prepared CNT sheets used in this study are already substantially conductive. In particular, the FTS doping effect on metallic nanotubes should be negligible given their very high carrier density, while the relative effect on pure semiconducting tubes should be much greater. Indeed, we have observed that conductivity of other CNT samples, mainly composed of single wall carbon nanotubes (SWCNT) with about 2/3 of semiconducting tubes and 1/3 of metallic ones, increased by a factor of 4 (by 300%) upon FTS doping.

Carrier concentration, n, in our aligned CNT sheets can be estimated by using the relationship, $\sigma = \mathbf{e}n \times \mu$, where $\mathbf{e}$ is the elementary charge, which for pristine CNT sheets with a mobility of $\sim 100\,\mathrm{cm^2V^{-1}s^{-1}}$ gives $n \approx 3 \times 10^{14}\,\mathrm{cm^{-2}}$. Assuming that mobility does not drastically change with FTS treatment, we can estimate the FTS-induced carrier concentration, $\Delta n \approx 1.88 \times 10^{14}\,\mathrm{cm^{-2}}$ for the conductivity increase of 60%. Such doping level is greater, in the sense of absolute numbers, than what we observed in other carbon based system (typically around $\sim 10^{13}\,\mathrm{cm^{-2}}$).[11–13] This difference might originate from: (a) errors associated with the application of the relationship $\sigma = \mathbf{e}n \times \mu$ to an inhomogeneous conductor (sparse CNT network), or (b) the unique highly porous morphology of densified CNT films that have a finite thickness and, contrary to impermeable solid surfaces, present a very high surface to volume ratio, so that n estimated in our measurements is a projected (areal) carrier density. Thus, we should keep in mind that the areal carrier density estimated above is associated with a bulk doping of the CNT layers, and strictly speaking it cannot be directly compared with the carrier density in intrinsically two-dimensional, impermeable systems. The above numbers can only be used for evaluation and comparison of the conductivity per square of large-area macroscopic electrodes.

Figures 3(b) and 3(c) are the scanning electron microscope (SEM) images of pristine and FTS-coated CNT sheets, respectively. The bright white areas in pristine CNTs (Fig. 3(b)) are the voids, through which an insulating glass substrate is "seen". It is obvious that CNT bundles are very sparse are clearly visible due to the significant difference between conductivities of the bundles and the glass, which results in a very high contrast of the SEM image of pristine CNT sample (Fig. 3(b)). After FTS treatment however, the contrast becomes much smaller, since now both the glass and the nanotube bundles are coated with a dense insulating nanoscale membrane—the monolayer of FTS, with the inert perfluorinated tails of SAM molecules pointing outwards. Such a contrast change appeared in all our tests, offering independent evidence that FTS vapor penetrates through the entire thickness of CNT layer and effectively coats individual bundles. We also note that there is no noticeable change in the visual appearance, color or optical transparency of the CNT sheets after FTS doping.

Finally, we note that the observed FTS doping of CNTs is stable, as long as the samples are kept either in high vacuum or in an atmosphere of non-polar gases. In prolonged and repetitive tests after the FTS deposition, no significant degradation of conductivity has been detected. Some of the FTS-doped samples have been stored in vacuum-sealed plastic packages for about a year, after which the tests showed that the high conductivity level induced by FTS remained.

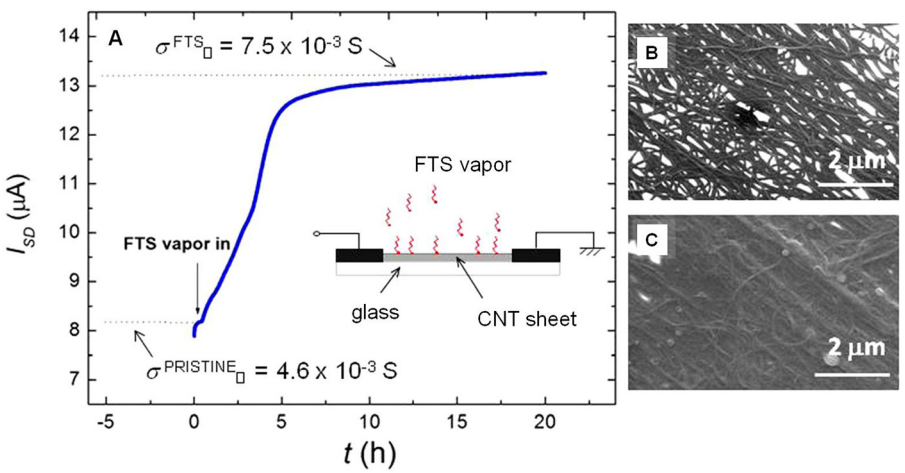

FIG. 3. (a) The current flowing through an ungated partially aligned CNT sheet as a function of time during the exposure to FTS vapor ($V = 10\,\mathrm{mV}$). The vertical arrow indicates the time when FTS vapor has been introduced into the vacuum chamber. The sheet conductivities, $\sigma^{PRISTINE}$ and σ^{FTS}, are the values determined using the effective width, W_{eff}, of the CNT film as discussed in the text. The inset is a sketch of the sample. (b) and (c) are SEM images of CNT sample before and after the FTS growth, respectively. The clear change of the SEM contrast after FTS deposition is observed systematically and appears to be an intrinsic effect of FTS coating.

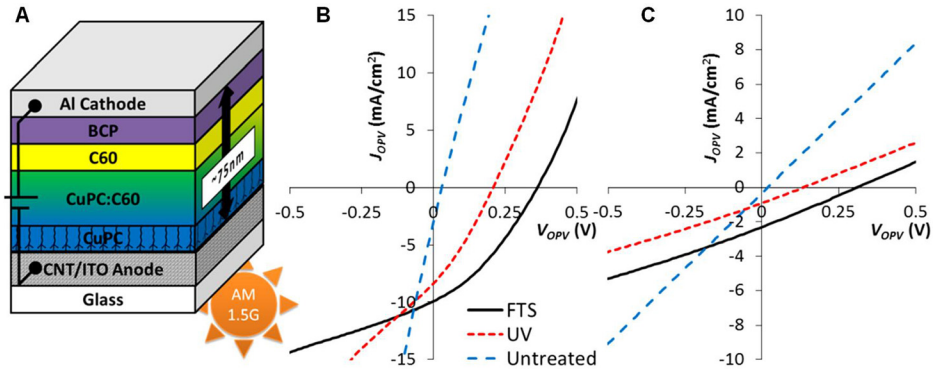

FIG. 4. **Organic photovoltaic cells with CNT-based anodes: the effect of FTS doping of the anode.** (a) Device structure of the OPV cell. (b) Current-voltage characteristics for devices with an anode composed of a thin CNT layer deposited on ITO. (c) Current-voltage characteristics for devices with CNT only anodes. Different curves compare the performance of devices with untreated anodes (long dashed line) and anodes treated with FTS (solid line) or UV-Ozone (short dashed line).

D. Organic solar cell devices with FTS doped CNT contacts

As a demonstration of the practical utility of FTS doping, we have fabricated organic photovoltaic devices (OPV) with FTS doped CNT electrodes. The device structure is depicted in Fig. 4(a). This structure employs a co-deposited CuPc:C60 active layer in a design similar to that reported by Sullivan *et al.*[18] Two different anode configurations were tested: one in which a thin layer of SWCNT fabricated by Canatu Corp. as described in Ref. 19 was laid onto ITO (CNT/ITO anode) and a second in which a thicker layer of CNT, also from Canatu Corp., was used alone (CNT-only anode). The CNT/ITO anode has a relatively constant conductivity regardless of doping treatment due to the already high conductivity of ITO, but the resistance of the CNT-only anode is greatly improved by FTS doping as demonstrated above. We compared the performance of OPV devices with no treatment of anode, FTS treatment, and UV-Ozone treatment (Figs. 4(b) and 4(c)). To limit experimental variations between different devices, each device contained two pixels of each electrode configuration, and all devices were fabricated with the same organic layer deposition. Without any treatment, these thin devices show poor current rectification and other diode characteristics, which is a result of CNT bundles protruding through the active layer. Upon FTS doping, we expected to see a moderate improvement in the filling factor (FF) and short circuit current (J_{SC}) in the CNT-only device and little effect on the CNT/ITO device. However, we observed significant improvements of the performance of both devices. Furthermore, UV-Ozone treatment of the anode shows a qualitatively similar effect as the FTS treatment, but the FTS treatment leads to a much stronger improvement of solar cell parameters (Fig. 4).

These results are surprising as the improvement in device performance appears to be due to a large *increase* of the shunt resistance of these devices, rather than the expected decrease in the series resistance. The shunt resistance is related to a parasitic leakage current through the active semiconducting layer, while the device is under reverse bias. Increased shunt resistance, which is highly desirable in OPVs, suggests that there is less shunting of charges through the thin active layer by protruding CNT bundles. Possible explanations include an increase in effective work function of the CNTs, the FTS forming an electron blocking layer, or ablation of protruding tips of the CNTs.

The similar tendency of improved *J-V* characteristics for FTS and UV-Ozone treatments suggests that the effect could be due to an increase of the anode's work function, as it is well known that UV-Ozone treatment increases the work function of CNTs through oxygen incorporation and *p*-type doping.[20,21] It is also possible that in the case of FTS treated CNT anode, a conformal FTS monolayer creates a nanoscale insulating barrier between the CNT bundles and the organic semiconductor. The conformal nature of FTS growth on organic surfaces is known.[11,12] It is also evident from the uniform and homogeneous change of contrast in SEM images of CNTs before and after the FTS treatment (Figs. 3(b) and 3(c)). Such an insulating conformal monolayer might greatly reduce shorts caused by individual protruding CNT bundles, leading to a higher shunt resistance of the OPV device. Yet, it is not significantly resistive to increase the series resistance of the device in the forward bias. Thus, both *p*-type doping of the CNT anode and an increased shunt resistance by FTS coating are likely the causes of the observed performance improvement in our OPV cells.

III. CONCLUSIONS

In conclusion, we have successfully fabricated top-gated field effect transistors on aligned carbon nanotube sheets using a conformal (parylene) polymer gate insulator. The field effect mobility and the density of charge carriers in pristine CNT sheets were estimated to be $\sim 100\,cm^2V^{-1}s^{-1}$ and 3×10^{14} cm^{-2}, respectively. We have demonstrated that CNT sheets can be strongly *p*-doped by coating with a self-assembled monolayer of *fluoroalkyl trichlorosilane*, leading to a 60–300% increase in the sheet conductivity of the CNT films (with the actual relative doping level depending on the initial sample's conductivity). The corresponding projected areal density of FTS-induced carriers was estimated to be around 1.8×10^{14} cm^{-2}. We have observed significant improvements in performance of OPV devices that utilize CNT anodes functionalized with FTS. Such a strong and stable doping is very promising for boosting CNT applications as transparent electrodes for organic and flexible electronics.

ACKNOWLEDGMENTS

This work has been financially supported by NSF ARRA CAREER award under Grant No. NSF-DMR-0843985.

[1]K. H. An, S. Y. Jeong, H. R. Hwang, and Y. H. Lee, "Enhanced sensitivity of a gas sensor incorporating single-walled carbon nanotube-polypyrrole nanocomposites," Adv. Mater. **16**, 1005–1009 (2004).
[2]E. Bekyarova *et al.*, "Chemically functionalized single-walled carbon nanotubes as ammonia sensors," J. Phys. Chem. B **108**, 19717–19720 (2004).
[3]D. S. Hecht *et al.*, "Bioinspired detection of light using a porphyrin-sensitized single-walled nanotube field effect transistor," Nano Lett. **6**, 2031–2036 (2006).
[4]R. Ulbricht *et al.*, "Transparent carbon nanotube sheets as 3-D charge collectors in organic solar cells," Solar Energy Mater.Solar Cells **91**, 416–419 (2007).
[5]E. S. Snow, J. P. Novak, P. M. Campbell, and D. Park, "Random networks of carbon nanotubes as an electronic material," Appl. Phys. Lett. **82**, 2145–2147 (2003).
[6]E. Artukovic, M. Kaempgen, D. S. Hecht, S. Roth, and G.Grüner, "Transparent and flexible carbon nanotube transistors," Nano Lett. **5**, 757–760 (2005).
[7]H. E. Unalan, G. Fanchini, A. Kanwal, A. Du Pasquier, and M. Chhowalla, "Design criteria for transparent single-wall carbon nanotube thin-film transistors," Nano Lett. **6**, 677–682 (2006).
[8]C. Kocabas *et al.*, "Experimental and theoretical studies of transparent through large scale, partially aligned arrays of single-walled carbon nanotubes in thin film type transistors," Nano Lett. **7**, 1195–1202 (2007).
[9]S. J. Kang *et al.*, "High-performance electronics using dense, perfectly aligned arrays of single-walled carbon nanotubes," Nat. Nanotech. **2**, 230–236 (2007).
[10]M. Zhang, S. Fang, A. A. Zakhidov, S. B. Lee, A. E. Aliev, C. D. Williams, K. R. Atkinson, and R. H. Baughman, "Strong, transparent, multifunctional, carbon nanotube sheets," Science **309**, 1215–1219 (2005).
[11]M. F. Calhoun, J. Sanchez, D. Olaya, M. E. Gershenson, and V. Podzorov, "Electronic functionalization of the surface of organic semiconductors with self-assembled monolayers," Nat. Mater. **7**, 84–89 (2008).
[12]C.-Y. Kao *et al.*, "Doping of conjugated polythiophenes with alkyl silanes," Adv. Funct. Mater. **19**, 1906–1911 (2009).
[13]B. Lee, Y. Chen, F. Duerr, D. Mastrogiovanni, E. Garfunkel, E. Y. Andrei, and V. Podzorov, "Modification of electronic properties of graphene with self-assembled monolayers," Nano Lett. **10**, 2427–2432 (2010).
[14]V. Podzorov, V. M. Pudalov, and M. E. Gershenson, "Field-effect transistors on rubrene single crystals with parylene gate insulator," Appl. Phys. Lett. **82**, 1739–1741 (2003).
[15]M. S. Fuhrer, B. M. Kim, T. Dürkop, and T. Brintlinger, "High-mobility nanotube transistor memory," Nano Lett. **2**, 755–759 (2002).
[16]M. Radosavljević, M. Freitag, K. V. Thadani, and A. T. Johnson, "Nonvolatile molecular memory elements based on ambipolar nanotube field effect transistors," Nano Lett. **2**, 761–764 (2002).
[17]J. B. Cui, R. Sordan, M. Burghard, and K. Kern, "Carbon nanotube memory devices of high charge storage stability," Appl. Phys. Lett. **81**, 3260–3262 (2002).
[18]P. Sullivan, S. Heutz, S. M. Schultes, and T. S. Jones, "Influence of codeposition on the performance of CuPc–C_{60} heterojunction photovoltaic devices," Appl. Phys. Lett. **84**, 1210–1212 (2004).
[19]A. Kaskela *et al.*, "Aerosol-synthesized SWCNT networks with tunable conductivity and transparency by a dry transfer technique," Nano Lett. **10**, 4349–4355 (2010).
[20]J. Xue, "Carrier transport in multilayer organic photodetectors: II. Effects of anode preparation," J. Appl. Phys. **95**, 1869–1877 (2004).
[21]D. Kang, N. Park, J. Ko, E. Bae, and W. Park, "Oxygen-induced p-type doping of a long individual single-walled carbon nanotube," Nanotechnology **16**, 1048–1052 (2005).